

# SUPPORTING INFORMATION

## Nitrogen Oxidation in a Multi-Pin Plasma System in the Presence and Absence of a Plasma/Liquid Interface

Moazameh Adhami Sayad Mahaleh <sup>1</sup>, Mehrnoush Narimisa <sup>1</sup>, Anton Nikiforov <sup>1</sup>, Mikhail Gromov <sup>1,\*</sup>, Yury Gorbanev <sup>2</sup>, Rim Bitar <sup>1</sup>, Rino Morent <sup>1</sup> and Nathalie De Geyter <sup>1</sup>

<sup>1</sup> Research Unit Plasma Technology (RUPT), Department of Applied Physics, Ghent University, Sint-Pietersnieuwstraat 41, 9000 Ghent, Belgium; moazameh.adhamisayadmahaleh@ugent.be (M.A.S.M.); mehrnoush.narimisa@ugent.be (M.N.); anton.nikiforov@ugent.be (A.N.); rim.bitar@ugent.be (R.B.); rino.morent@ugent.be (R.M.); nathalie.degeyter@ugent.be (N.D.G.)

<sup>2</sup> Research Group PLASMANT, Department of Chemistry, University of Antwerp, Universiteitsplein 1, 2610 Wilrijk, Belgium; yury.gorbanev@uantwerpen.be

\* Correspondence: mikhail.gromov@ugent.be

## 1. Electrical circuit

The electrical circuit of the pulsed forming network is presented in Figure S1. A main capacitor ( $C_1$ , 1.3 nF) was used as energy storage together with a resistor ( $R_1$ , 1.8 k $\Omega$ ) which limited the total current passing from the DC power supply. When the capacitor  $C_1$  was charged to a voltage which was sufficiently high to break down the gas in the main spark gap, simultaneous discharges took place between the pins and the ground electrode (metal or liquid) and the capacitor  $C_1$  was discharged through the parallel RC circuits ( $R_2$ , 1 M $\Omega$ ;  $C_2$ , 10 pF). It is important to note that a parallel RC circuit ( $R_2$ , 1 M $\Omega$ ;  $C_2$ , 10 pF) was connected to a multi-pin electrode system to distribute equivalently the pulse energy between all pins and to provide a relaxation time  $1/RC$  above  $10^{-4}$  s for fast discharge operation in the form of streamers.

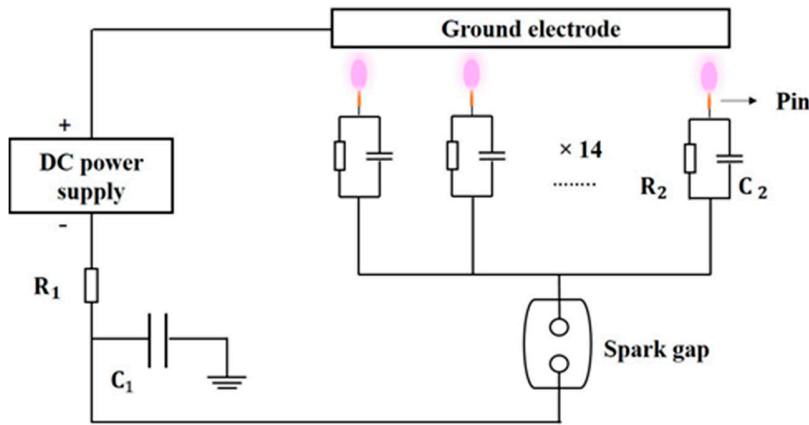


**Figure S1.** Electrical circuit of the pulsed plasma generator.

## 2. Griess assay

To form the Griess reagent (100 mL), 1 g sulphanilic acid, 0.1 g naphthylenediamine and 2.3 mL phosphoric acid (85%) were added to 97.7 mL of distilled water. After plasma exposure under different operational parameters, 1 mL of the Griess reagent was added to 1 mL of plasma exposed liquid sample. The mix of the Griess reagent and the sample was kept in the dark for 10 min thereby developing a pink color. Afterwards, the nitrite concentration inside the liquid sample was determined by recording an absorption spectrum using a Shimadzu mini 1240 spectrometer in the spectral range  $\lambda=400-700$  nm.

## 3. Calculation of the energy cost

The energy cost was calculated as follows:

$$EC_{N-fixed} [MJ/mol] = \frac{P [W]}{\text{moles of fixed N produced per second } [mol s^{-1}]} \cdot \frac{1}{10^6 [J/MJ]} \quad (1)$$

where P is the plasma power in [W]. The moles of the fixed N produced per second were determined as a sum of all nitrogen-containing products detected in the gas and liquid phases:

$$\text{moles of fixed N produced per second in the gas phase [mol s}^{-1}] = \frac{C_{NO_x}[\text{ppm}] \cdot 10^{-6} \cdot Q[\text{L s}^{-1}]}{V_{\text{molar}}[\text{L mol}^{-1}]} \quad (2)$$

$$\text{moles of fixed N produced per second in the liquid phase [mol s}^{-1}] = \frac{C_{NO_x^-}[\text{mol L}^{-1}] \cdot V[\text{L}]}{t[\text{s}]} \quad (3)$$

where C is the concentration of  $NO_x$  and  $NO_x^-$  in the gas [ppm] and liquid [mol L<sup>-1</sup>] phases, Q is the gas flow rate [L s<sup>-1</sup>],  $V_{\text{molar}}$  is the molar volume [L mol<sup>-1</sup>], V is the volume of the liquid phase [L], and t is the plasma treatment time [s] after which the sample was analyzed.

#### 4. Plasma voltage waveform

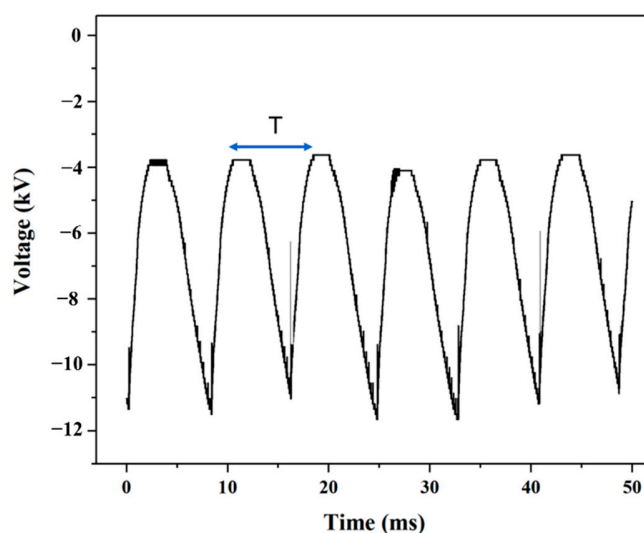


**Figure S2.** Voltage curve as a function of time for a plasma power of 20 W and a gas flow rate of 4 L min<sup>-1</sup>. T represents the plasma period.

#### 5. Gas temperature, plasma frequency, electron density and occurring chemical reactions

Figure S3 illustrates an example of the curve fitting using MassiveOES software for the Me-Me configuration at a discharge power of  $90 \pm 2$  W and a gas flow rate of 4 L min<sup>-1</sup>. Under these experimental conditions, the rotational temperature and the vibrational temperature was found to be  $1280 \pm 16$  and  $3825 \pm 27$  K, respectively.

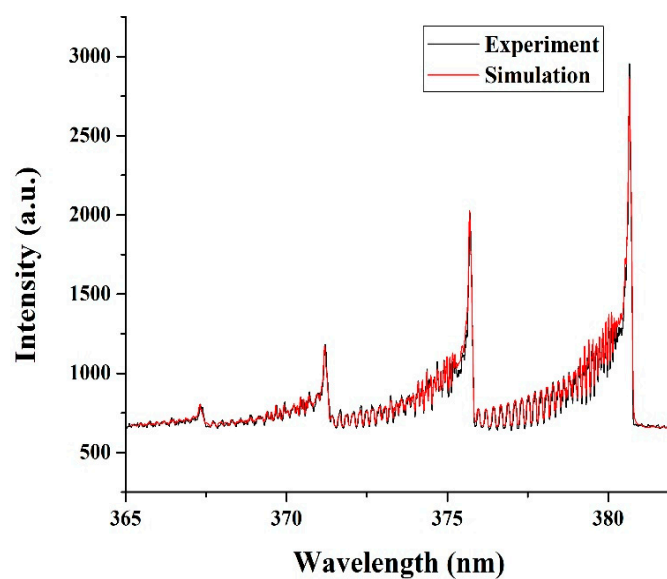


**Figure S3.** Example of MassiveOES simulation of the OES spectrum of the Me-Me electrode system for a gas flow rate of  $4 \text{ L min}^{-1}$  and a discharge power of  $90 \pm 2 \text{ W}$ .

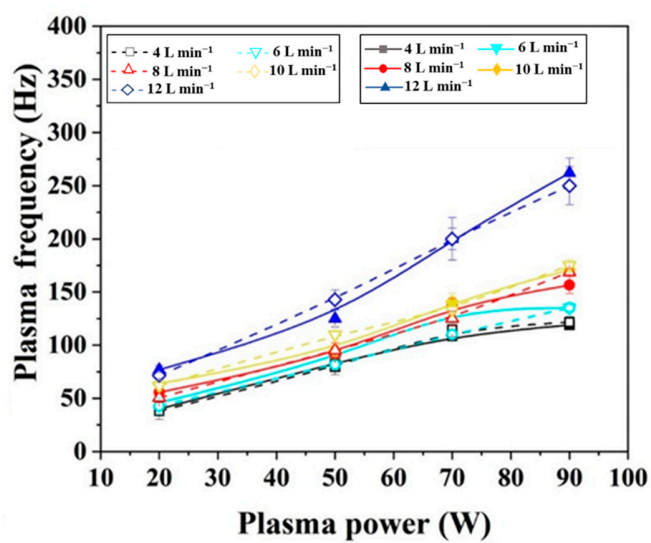


**Figure S4.** Discharge frequency variation in the chopping gap as a function of power for the different flow rates under study in the Me-Me and Me-L systems.

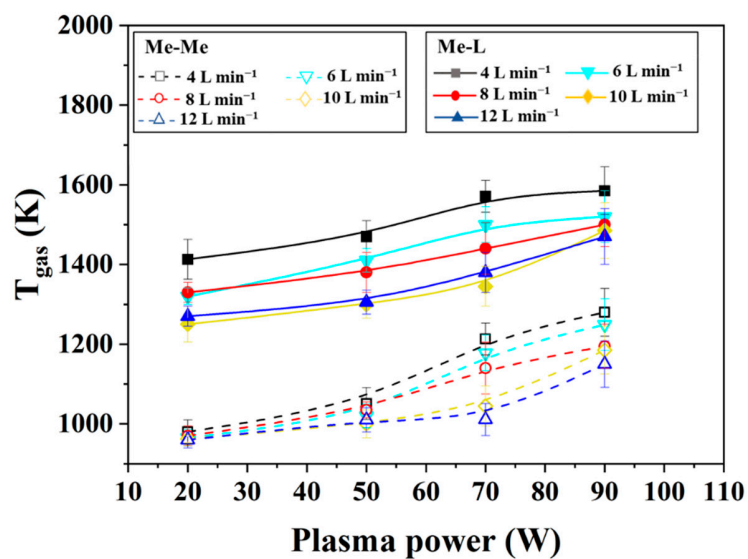


**Figure S5.** Gas temperature as a function of plasma power for the different flow rates under study in the Me-Me and Me-L systems.

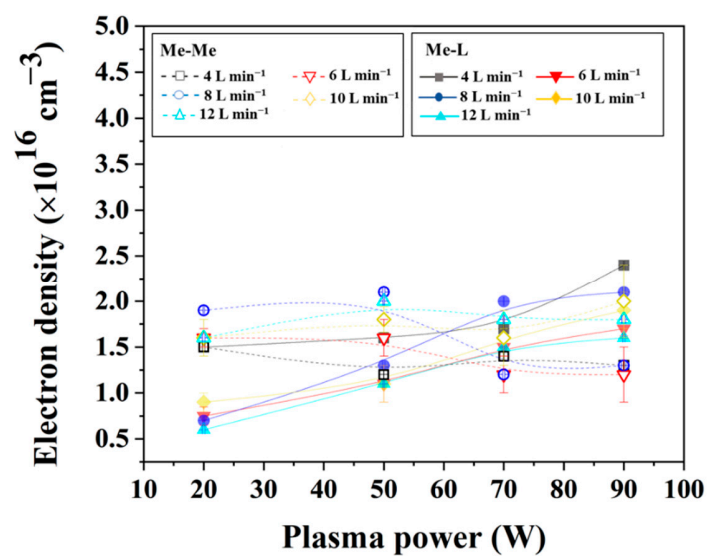


**Figure S6.** Estimated electron density as a function of plasma power for the different flow rates under study in the Me-Me and Me-L systems.

**Table S1.** Possible chemical reactions occurring in the gas and liquid phases.

Reaction	Coefficient rate	Ref
$^a\text{N}_2^* + \text{O} \rightarrow \text{NO} + \text{N}^*$	$7 \times 10^{-18}$	[39]
$\text{N}^* + \text{O}_2 \rightarrow \text{NO} + \text{O}^*$	$9 \times 10^{-19}$ - $3.3 \times 10^{-18}$	[39]
$\text{N} + \text{O} + ^\dagger\text{M} \rightarrow \text{NO} + \text{M}$	$5.6 \times 10^{-39}$	[39]
$\text{N} + \text{OH} \rightarrow \text{NO} + \text{H}$	$3.8 \times 10^{-17}$	[39,40]
$\text{O}_2 + \text{O} + \text{M} \rightarrow \text{O}_3 + \text{M}$	$3 \times 10^{-10}$	[39,40]
$\text{NO} + \text{O}_3 \rightarrow \text{NO}_2 + \text{O}_2$	$3.16 \times 10^{-12}$	[39,40]
$\text{NO} + \text{O} + \text{M} \rightarrow \text{NO}_2 + \text{M}$	$1.03 \times 10^{-30} \ddagger$	[39]
$\text{NO} + \text{N}_2\text{O} \rightarrow \text{N}_2 + \text{NO}_2$	$1.9 \times 10^{-10}$	[41]
$\text{HO}_2 + \text{NO}_2 \rightarrow \text{HNO}_2 + \text{O}_2$	$1.20 \times 10^{-13}$	[41]
$\text{H}_2\text{O} + \text{NO}_2 \rightarrow \text{HNO}_2 + \text{OH}$	$1.35 \times 10^{-11}$	[13]
$\text{OH} + \text{NO} + \text{N}_2 \rightarrow \text{HNO}_2 + \text{N}_2$	$7.40 \times 10^{-31} \ddagger$	[42]
$\text{OH} + \text{NO} + \text{O}_2 \rightarrow \text{HNO}_2 + \text{O}_2$	$7.40 \times 10^{-31} \ddagger$	[42]
$\text{HNO}_2 + \text{OH} \rightarrow \text{NO}_2 + \text{H}_2\text{O}$	$5.95 \times 10^{-12}$	[43]
$\text{NO}_2 + \text{HNO} \rightarrow \text{HNO}_2 + \text{NO}$	$1 \times 10^{-13}$	[44]
$\text{OH} + \text{NO} \rightarrow \text{HNO}_2$	$1.78 \times 10^{-11}$	[13]
$\text{HO}_2 + \text{NO}_2 \rightarrow \text{HNO}_2 + \text{O}_2$	$1.2 \times 10^{-13}$	[43]
$\text{NO}(\text{g}) + \text{H}_2\text{O}(\text{aq}) \rightarrow \text{NO}(\text{aq}) + \text{H}_2\text{O}(\text{aq})$	$4.4 \times 10^{-2}$	[39]
$\text{NO}_2(\text{g}) + \text{H}_2\text{O}(\text{aq}) \rightarrow \text{NO}_2(\text{aq}) + \text{H}_2\text{O}(\text{aq})$	$2.8 \times 10^{-1}$	[39]
$\text{HNO}_2(\text{g}) + \text{H}_2\text{O}(\text{aq}) \rightarrow \text{HNO}_2(\text{aq}) + \text{H}_2\text{O}(\text{aq})$	$1.15 \times 10^3$	[39]
$\text{OH}(\text{g}) + \text{H}_2\text{O}(\text{aq}) \rightarrow \text{OH}(\text{aq}) + \text{H}_2\text{O}(\text{aq})$	$6.2 \times 10^2$	[39]
$\text{OH}_2(\text{g}) + \text{H}_2\text{O}(\text{aq}) \rightarrow \text{OH}_2(\text{aq}) + \text{H}_2\text{O}(\text{aq})$	$1.3 \times 10^5$	[39]
$\text{NO} + \text{NO}_2 + \text{H}_2\text{O} \rightarrow 2\text{NO}_2^- + 2\text{H}^+$	$1.2 \times 10^{13} \ddagger\ddagger$	[45]
$2\text{NO}_2 + \text{H}_2\text{O} \rightarrow \text{NO}_2^- + \text{NO}_3^- + 2\text{H}^+$	$2 \times 10^{14}$	[45]
$\text{HNO}_2 + \text{H}_2\text{O} \rightarrow \text{NO}_2^- + \text{H}^+$	$1.8 \times 10^7$	[46]
$\text{OH} + \text{NO} \rightarrow \text{HNO}_2$	$2 \times 10^{16}$	[46]
$\text{NO} + \text{OH}_2 \rightarrow \text{HNO}_3$	$2 \times 10^{15}$	[46]
$\text{NO}_2 + \text{OH} \rightarrow \text{HNO}_3$	$3 \times 10^{16}$	[46]

† - M is O<sub>2</sub> or N<sub>2</sub>.

<sup>a</sup>- The electronically and vibrationally excited states of N<sub>2</sub> ( $A^3 \Sigma_u^+$ ,  $B^3 \Pi_g$ ,  $C^3 \Pi_u$ ,  $X^1 \Sigma_g^+(v > 12)$ ).

‡ - Three body reactions in the gas phase with the reaction rate in m<sup>6</sup>s<sup>-1</sup>; and ‡‡ three body reactions in the liquid phase with reaction rate in M<sup>-2</sup>s<sup>-1</sup>.

## 6. Evolution of NO and NO<sub>2</sub> concentrations and energy cost of the discharge

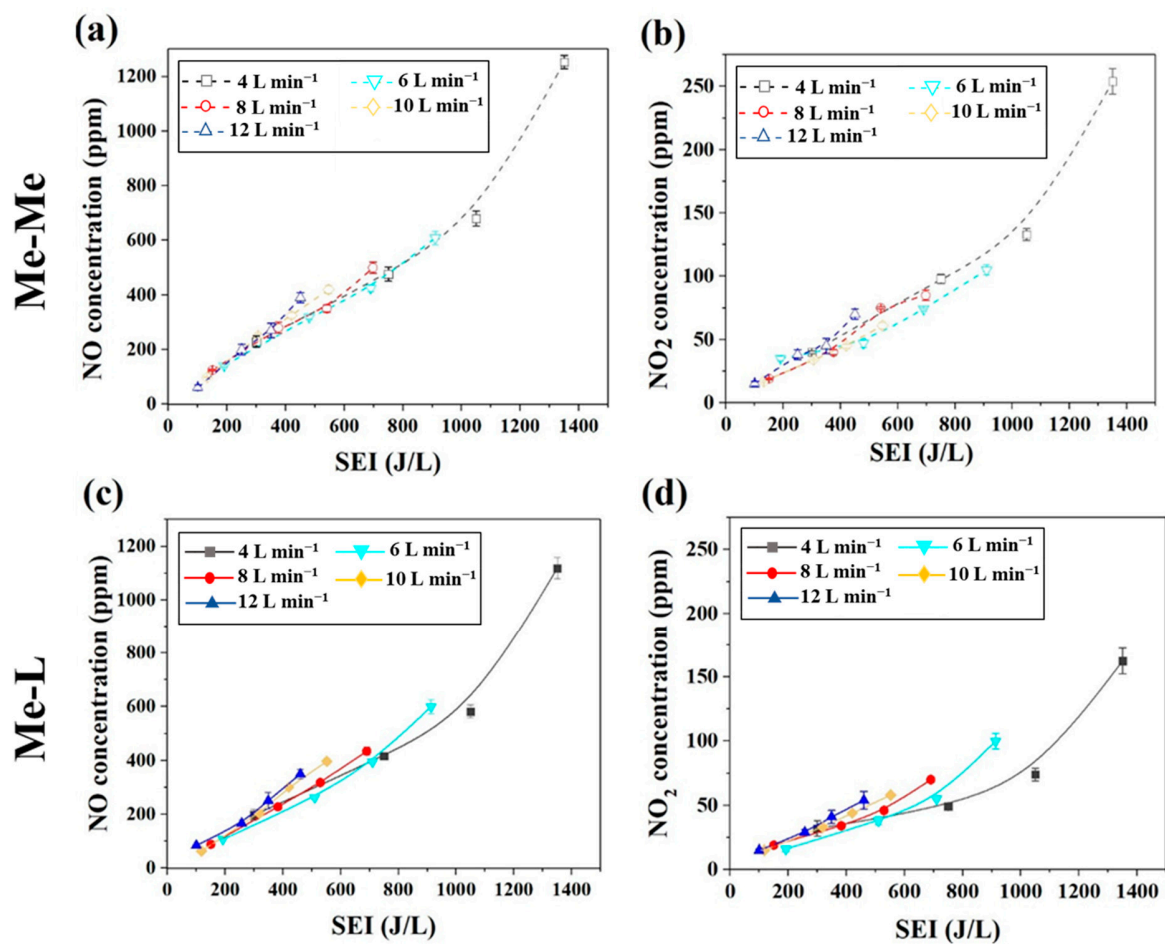


**Figure S7.** (a), (c) NO, and (b), (d) NO<sub>2</sub> concentrations as a function of SEI for different gas flow rates for the Me-Me and Me-L systems.

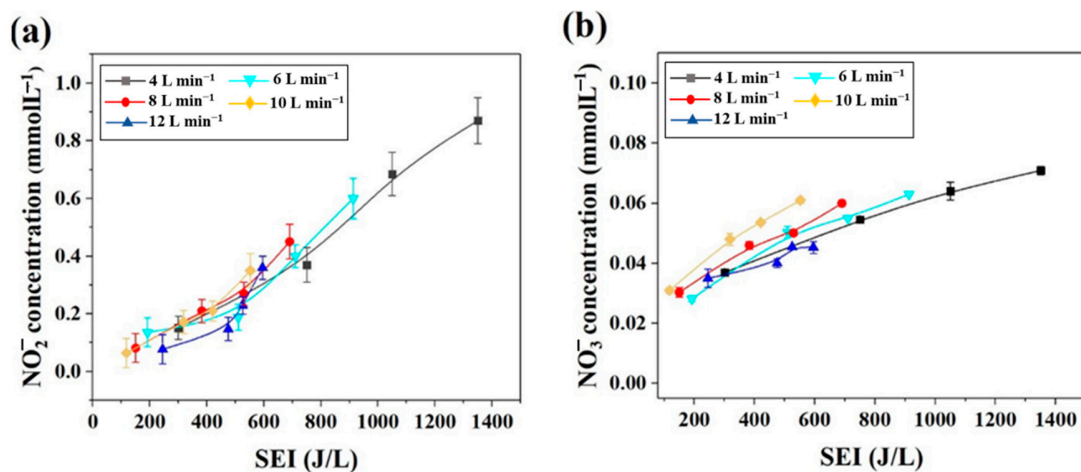


**Figure S8.** Evolution of (a) nitrite and (b) nitrate concentrations generated in the liquid phase as a function of SEI in different gas flow rates for the Me-L system.

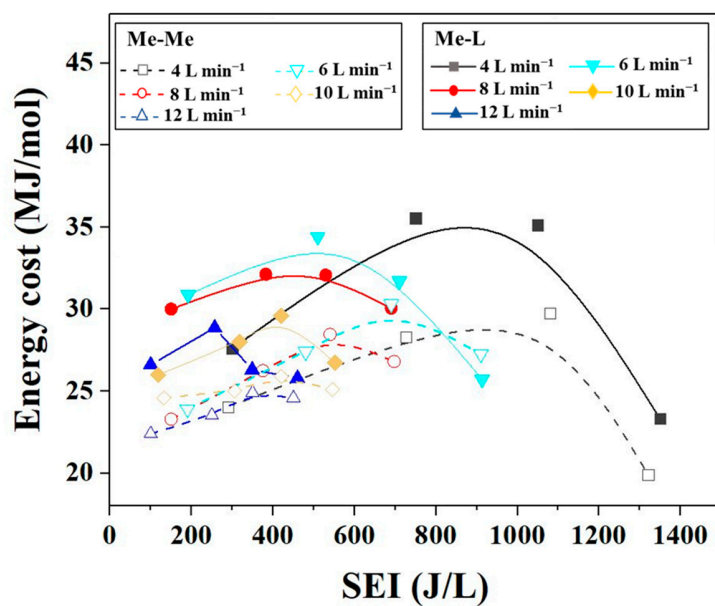


**Figure S9.** Energy cost of the pulsed discharge as a function of SEI for different gas flow rates in both electrode configurations.